Available online at www.sciencedirect.com
SCIENCE DIRECT®

Spectrochimica Acta Part A 61 (2005) 1933–1938

SPECTROCHIMICA ACTA
PART A

www.elsevier.com/locate/saa

Optical poling effect and optical absorption of cyan, ethylcarboxyl and *tert*-buthyl derivatives of 1H-pyrazolo[3,4-b]quinoline: experiment and quantum–chemical simulations

E. Koścień[a], J. Sanetra[b], E. Gondek[b], B. Jarosz[c], I.V. Kityk[d], J. Ebothe[e], A.V. Kityk[a,*]

[a] *Institute for Computer Science, Technical University of Czestochowa, Armii Krajowej 17, 42-200 Czestochowa, Poland*
[b] *Institute of Physics, Technical University of Krakow, Podhorazych 1, 30-084 Krakow, Poland*
[c] *Department of Chemistry, Hugon Kołłotaj Agricultural University, Al. Mickiewicza 24/28, 30-059 Krakow, Poland*
[d] *Institute of Biology and Biophysics, Technical University of Czestochowa, PL-42200 Czestochowa, Poland*
[c] *Universite de Reims, UTAP-LMET, EA No 2061, UFR Sciences, Boite Postale 138, 21 Rue Clement Ader, Reims, France*

Received 2 July 2004; accepted 28 July 2004

Abstract

We present here results of experimental studies and quantum–chemical simulations of optical absorption and optical poling effects performed on a new synthesized cyan, ethylcarboxyl and *tert*-buthyl derivatives of 1H-pyrazolo[3,4-b]quinoline incorporated into polymer matrix or dissolved in organic solutions. The efficiency of second-order optical susceptibility d vs photoinduced power density I_p clearly saturates to certain magnitude d_{eff} at sufficient power densities ($I_p \geq 1.3\,\mathrm{GW\,cm^{-2}}$). Comparing experimental data and results of semiempirical quantum–chemical simulations one can conclude that there exists generally a good correlation between the magnitude of saturated susceptibilities d_{eff} and macroscopic hyperpolarizabilities for all compounds except the chromophore 1,3-dimethyl-6-cyano-[PQ] only. The discrepancy for this compound may reflect a specific contribution of surrounding polymer matrix. According to the quantum chemical analysis the methyl-containing cyan and ethylocarcoxyl derivatives reveal four/five strong absorption bands in the spectral range 200–500 nm. A substitution of the methyl groups by the phenyl group causes the substantial changes of the absorption spectra mainly in the spectral range 240–370 nm. Measured and calculated absorption spectra manifest rather good agreement mainly in the part regarding the spectral positions of the first oscillator (absorption threshold). The quantum–chemical PM3 method shows the best agreement with experiment. At the same time a considerable broadening almost of all absorption bands appears as a characteristic feature of all measured spectra. The discrepancies between the calculated and the measured spectra are attributed to electron–vibronic coupling as well as to a specific rotational dynamics of phenyl rings.

PACS: 33.20.Lg; 33.20.Kf; 33.70.-w; 42.70.Ky

Keywords: Organic materials; Visible and ultraviolet spectra; Optical poling; Optical second harmonic generation (SHG)

1. Introduction

Long illumination of an isotropic medium, such as glasses or polymers, by two mutually coherent sources with different frequencies (ω and 2ω) results in the accumulation of the reversible long-lived static polarization inside the medium [1–3]. The magnitude of the polarization is determined by the formation of a spatially periodic electrostatic field. Due to the loss of the center of symmetry there appear the properties of a non-centrosymmetric uniaxial medium with a photoinduced optical axes determined by the light polarization of the pumping beam. As a result, the optically induced second harmonic generation (SHG) and parametric amplification become possible in such perturbed medium. Optical poling is thereby a relatively new and quite effective technique providing an important information about second-order optical properties of disordered materials.

---

[*] Corresponding author. Tel.: +48 34 3250 838; fax: +48 34 3250 823.
E-mail address: kityk@ap.univie.ac.at (A.V. Kityk).

1386-1425/$ – see front matter © 2004 Elsevier B.V. All rights reserved.
doi:10.1016/j.saa.2004.07.025

The main purpose of the present work is the experimental studies of the optical absorption and optical poling effects of new synthesized cyan, ethylcarboxyl and *tert*-buthyl derivatives of 1H-pyrazolo[3,4-b]quinoline (hereafter referred as [PQ]) incorporated into polymer matrix or dissolved in organic solutions. The paper deals with the following organic semiconductors: 1,3-dimethyl-6-COOEt-1H-pyrazolo[3,4-b]quinoline (1,3-dimethyl-6-COOEt-[PQ]), 1,3-dimethyl-6-cyano-1H-pyrazolo[3,4-b]quinoline (1,3-dimethyl-6-cyano-[PQ]), 1-phenyl-3-methyl-6-COOEt-1H-pyrazolo[3,4-b]quinoline (1-phenyl-3-methyl-6-COOEt-[PQ]), 1-phenyl-3-methyl-6-cyano-1H-pyrazolo[3,4-b]quinoline (1-phenyl-3-methyl-6-cyano-[PQ]), 1-phenyl-3-methyl-6-t-buthyl-1H-pyrazolo[3,4-b]quinoline (1-phenyl-3-methyl-6-t-buthyl-[PQ]). The optical absorption and optical poling can be considered as the most appropriate methods to study the basic electronic properties of these materials. The absorption spectra in UV and visible regions give an important information about interacting conjugated π-electrons which obviously are also the basis of the relevant luminescent and electroluminescent properties of the organic materials. It is amazing that [PQ]-derivatives are known as a class of highly fluorescent materials in the blue spectral range [4] as well as promising materials for electroluminescent applications [5,6]. Since the origin of these effects are related much with molecular electron structure, the experimental results are supplied by quantum–chemical calculations. The quantum PM3 and AM1 method have been found as the most appropriate for simulations of the experimental data.

The optical properties of the [PQ]-derivative materials significantly depend on the pattern of substitution as well as on the type of substituents, as documented in several our recent publications [7,8]. In particular, a substitution of the methyl groups by at least one phenyl group causes the drastic changes of the absorption spectra mainly in the spectral range 240–370 nm. These differences are attributed to additional molecular double bounded conjugated segments C=C of the substituted phenyl groups i.e. to $\pi \rightarrow \pi^*$ transitions. The measured spectra demonstrate usually a considerable broadening almost of all absorption bands. The experiments performed with highly and weakly polar organic solvents [8] show that the solvatochromic effect on the absorption spectra is indeed small. For this reason the discrepancies between the calculated and the measured spectra have been attributed mainly to electron–vibronic coupling as well as to rotational dynamics of phenyl rings.

2. Synthesis and experimental

Depending on lateral substituants, several chemical compounds mentioned below were used for the synthesis of a particular [PQ]-derivative. All reagents were used as received from Aldrich or Fluka without further purification. Column chromatography was performed on Merck silica gel 60 (230–400 mesh) using toluene/ethyl acetate (3:1) as eluent. All the [PQ]-derivatives 3 were prepared according to procedures described in Ref. [9–12] by condensation of substituted aromatic amines 2 with 5-chloro-1,3-dimethyl- and 5-chloro-3-methyl-1-phenyl-1H-pyrazole-4-carbaldehydes 1 (see Scheme 1 and Table 1). As the result, the following compounds were synthesized for further optical studies: 1,3-dimethyl-6-COOEt-[PQ], 1,3-dimethyl-6-cyano-[PQ], 1-phenyl-3-methyl-6-COOEt-[PQ], 1-phenyl-3-methyl-6-cyano-[PQ] and 1-phenyl-3-methyl-6-*t*-buthyl-[PQ]. The purity of these compounds was checked by TLC (Merck). The optical absorption spectra were recorded in tetrahydrofuran solution (mass concentration of about 0.1%) using Shimadzu UV–vis 2101 scanning spectrophotometer in range 200–500 nm. The measurements were performed using standard 1 cm path length quartz cuvette for absorption spectrometry.

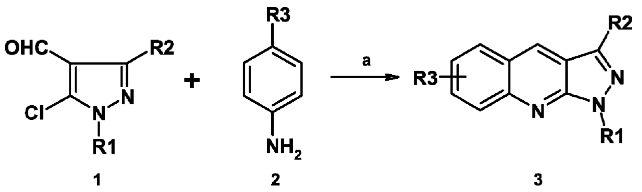

Scheme 1. Synthesis of the 1-H-pyrazolo[3,4-b]quinoline ([PQ]-) derivatives. Conditions: at the temperature of 140–190 °C within 30–60 min. The radicals R_1, R_2 and R_3 are mentioned in the Table 1.

The measurements of the optical second-order susceptibility have been performed in standard optical poling experiments. The experimental setup is shown in Fig. 1). As a fundamental laser source we have used Gd:YAG-laser generating at λ = 1.7 μm with pulse power P=21 MW and pulse duration about 30 ps. The laser beam is consequently split into two coherent beams by the beamsplitter BS. The second beam is converted by β-BBO crystal to a doubled-frequency signal (λ = 0.88 μm). Using two-channel scheme,

Table 1
Supplement to the Scheme 1: Chemical radicals R_1, R_2 and R_3

Compound	R_1	R_2	R_3
1,3-Dimethyl-6-COOEt-[PQ]	Me	Me	6-$COOC_2H_5$
1,3-Dimethyl-6-cyano-[PQ]	Me	Me	6-CN
1-Phenyl-3-methyl-6-COOEt-[PQ]	Ph	Me	6-$COOC_2H_5$
1-Phenyl-3-methyl-6-cyano-[PQ]	Ph	Me	6-CN
1-Phenyl-3-methyl-6-*t*-buthyl-[PQ]	Ph	Me	6-C_3H_9

[PQ], 1H-pyrazolo[3,4-b]quinoline.

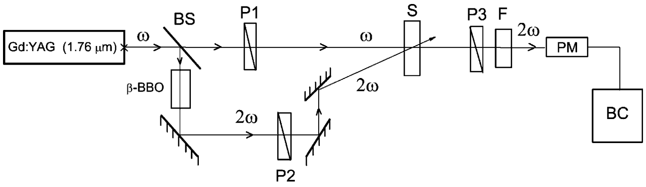

Fig. 1. The setup in optical poling experiment. BS is the beamsplitter; P1, P2 and P3 are the polarizers; S is the sample; F is the filter; PM is the photomultiplier; BC is the electronic boxcar.

we achieved the interaction of two coherent waves. We have found that coherence length is equal to about 28–36 μm. The observed output signal is detected by photomultiplier PM. Evaluation of the effective second-order susceptibility was done using a simple procedure described in the [13]. The investigated organic compounds were incorporated into the PMMA polymer matrices with weight concentration of about 5.5%.

3. Calculation procedure

The calculation of optical absorption spectra, static dipole moments and molecular second-order optical constants have been performed using the molecular dynamics quantum–chemical package Hyperchem 7.5. The geometrical optimization has been carried out by (MM+) force field method. Together with semi-empirical AM1 and PM3 methods this model is known to be as the most general and frequently used for molecular mechanics calculations developed principally for organic molecules. The calculations of optical absorption spectra and nonlinear susceptibility were consequently performed within several semi-empirical quantum–chemical models available in this software. However, the results will be presented for AM1 and parameterized PM3 methods, only. These methods indeed give the best agreement with the experiment. The optical spectra were calculated considering only the singly excited configuration interactions (CI); the excitation energies has been limited in both methods by the orbital criterion, i.e. to 12 occupied and 12 unoccupied orbitals.

The intensity of spectral optical absorption $I(\omega)$ is determined by the following expression (for details see e.g. [7,8]):

$$I(\omega) \approx \omega \sum_{k=1}^{n} \sum_{i=x,y,z} \frac{|<\Psi^{*}_{j_i}|i\hbar\vec{\nabla}_r|\Psi_{k_i}>|^2}{\hbar^2(\omega-\omega_{jk})^2+(\Gamma/2)^2} \qquad (1)$$

where Ψ_j and Ψ^{*}_k are wave functions of j-th and k-th energy levels and $i\hbar\vec{\nabla}_r$ is a transition dipole momentum operator of molecule, $\hbar\omega_{jk} = (E_j - E_k)$ is the energy difference between the ground and excited state, ω is the frequency of incident electromagnetic wave. Taking into account that the integration is performed over the space volume the intensity of spectral absorption then reads:

$$I(\omega) \approx \omega \sum_{k=1}^{n} \sum_{i=x,y,z} \frac{|(\mu)^{i}_{jk}|^2}{(\omega-\omega_{jk})^2+(\Gamma/2\hbar)^2}, \qquad (2)$$

where $(\mu)^{i}_{jk} = |<\Psi^{*}_{j_i}|\vec{\nabla}_r|\Psi_{k_i}>|$ are the transition dipole moments. It is necessary to emphasize that the resonance frequencies ω_{jk} and transition dipole momentum $(\mu)^{i}_{jk}$ have been obtained directly within PM3 and AM1 procedures, as described above. The empirical parameter Γ was chosen at magnitude of 0.12 eV, what gives the best agreement in lineshape of calculated optical absorption spectra compared to experimental data.

The molecular nonlinear hyperpolarizabilities β_{ijk} have been calculated using the model with so-called multilevel excitation [14]:

$$\begin{aligned}\beta_{ijk} = \frac{1}{8\hbar^2} \sum_{n',n,n'\neq n\neq g} \Bigg[& (\mu^{j}_{gn'} M^{i}_{n'n} \mu^{k}_{ng} + \mu^{k}_{gn'} M^{i}_{n'n} \mu^{j}_{ng}) \\ & \times \left(\frac{1}{(\omega_{n'g}-\omega)(\omega_{ng}+\omega)} + \frac{1}{(\omega_{n'g}+\omega)(\omega_{ng}-\omega)} \right) \\ & + (\mu^{i}_{gn'} M^{j}_{n'n} \mu^{k}_{ng} + \mu^{i}_{gn'} M^{k}_{n'n} \mu^{j}_{ng}) \\ & \times \left(\frac{1}{(\omega_{n'g}+2\omega)(\omega_{ng}+\omega)} + \frac{1}{(\omega_{n'g}-2\omega)(\omega_{ng}-\omega)} \right) \\ & + (\mu^{j}_{gn'} M^{k}_{n'n} \mu^{i}_{ng} + \mu^{k}_{gn'} M^{j}_{n'n} \mu^{i}_{ng}) \\ & \times \left(\frac{1}{(\omega_{n'g}-\omega)(\omega_{ng}+2\omega)} + \frac{1}{(\omega_{n'g}+\omega)(\omega_{ng}-2\omega)} \right) \Bigg] \end{aligned} \qquad (3)$$

where index gn(gn') means the transitions from the ground state g to excited state $n(n')$, $\omega_{n'g}$ and ω_{ng} are the corresponding transition frequencies; $M^{(x,y,z)}_{n'n} = (M^{(x,y,z)}_{gn'} - M^{(x,y,z)}_{gn})$, $M^{(x,y,z)}_{n'n}$ and $M^{(x,y,z)}_{n'n}$ are the excited state dipole components. Since the molecules in the polymer matrix are randomly oriented, the calculated second-order susceptibilities will be presented by its average (effective) magnitude $\beta_{av} = \sqrt{(\beta^2_{xxx} + \beta^2_{yyy} + \beta^2_{zzz})/3}$.

4. Experimental results and discussion

We start immediately with the analysis of optical absorption data. Measured spectra of 1,3-dimethyl-6-COOEt-[PQ], 1,3-dimethyl-6-cyano-[PQ], 1-phenyl-3-methyl-6-COOEt-[PQ], 1-phenyl-3-methyl-6-cyano-[PQ] and 1-phenyl-3-methyl-6-*t*-buthyl-[PQ] are presented in Figs. 2(a)–6(a), respectively, whereas the calculated absorption spectra (Γ = 0.12 eV) are shown in Figs. 2(b)–6(b). First two compounds of this list contain only methyl groups and their measured and calculated spectra are rather similar. The calculated spectra are characterized mainly by five or six relatively strong absorption bands. In particular one obtains for 1,3-dimethyl-6-COOEt-[PQ]: 394.5(370), 361(356), 292.5(282), 251(257), 239.5(233.5), 224(221) nm and for 1,3-dimethyl-6-cyano-[PQ]: 399(374.5), 365(358.5), 295(284.5), (258)251, 243(237.5), 226.5(222.5) nm as calculated by quantum–chemical PM3(AM1) methods. The corresponding experimental spectra (see Figs. 2(a) and 3(a)) have an absorption threshold at about 396 and 401 nm, respectively, which appears to be in fairly good agreement with quantum–chemical simulations, namely for absorption spectra calculated by PM3 method. The spectral positions of the strongest broad absorption band at about 268 and 252 nm (as for 1,3-dimethyl-6-COOEt-[PQ] and 1,3-dimethyl-6-cyano-

[PQ], respectively) in the measured spectra well coincide with the calculated spectra; PM3 method gives here again a bit better agreement. In addition, this absorption band of measured spectra is clearly asymmetric what let us to conclude that it appears as results of superposition of several overlapping unresolved broad spectral bands. Note, that quantum chemical calculations indeed shows in the same spectral region three relatively strong absorption bands for each compound.

Other three compounds, which represent the group of phenyl containing [PQ]-derivatives (see Figs. 4–6), show substantially different calculated spectra. The quantum–chemical simulations reveal here series of additional relatively strong absorption bands (from five up to seven ones) in the spectral range of 240–370 nm. Such feature is common for all [PQ]-derivatives containing phenyl groups as has been already shown (see e.g. [7,8]). An appropriate interpretation obviously refers to additional molecular doubled bonding segments C=C of the substituted phenyl groups. The absorption bands may be attributed in this case to $\pi \rightarrow \pi^*$ electronic transition from the bonding to anti-bonding molecular configuration. Total spectra of these organic compounds contain 8–11 relatively intense bands as one can realize from Figs. 4(b)–6(b). The measured absorption thresholds for all phenyl containing [PQ]-derivatives ($\lambda_g \approx 399$ nm) differ here slightly from those calculated by AM1(PM3) methods which give 406.5(373), 410(379) and 405(377.5) nm as calculated for 1-phenyl-3-methyl-6-COOEt-[PQ], 1-phenyl-

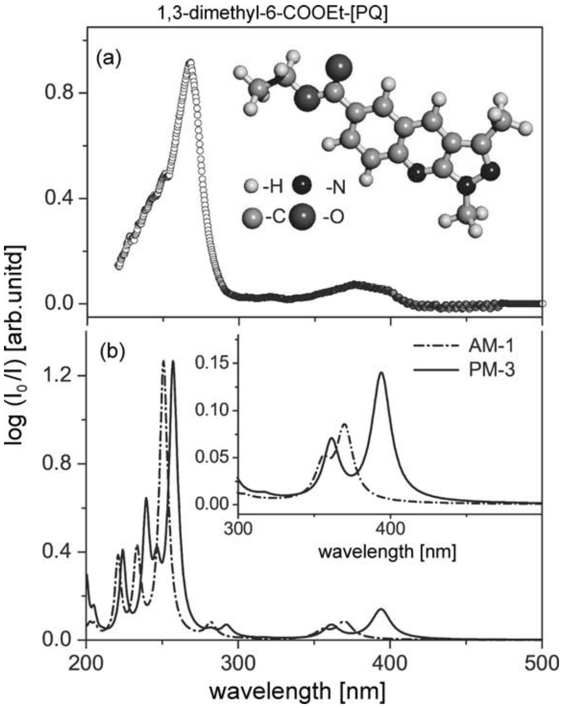

Fig. 2. (a) Measured absorption spectra of 1,3-dimethyl-6-COOEt-[PQ] and (b) calculated spectra within the semi-empirical quantum–chemical PM3 and AM1 models. Insert shows the chemical structure of 1,3-dimethyl-6-COOEt-[PQ] obtained within the geometrical optimization procedure.

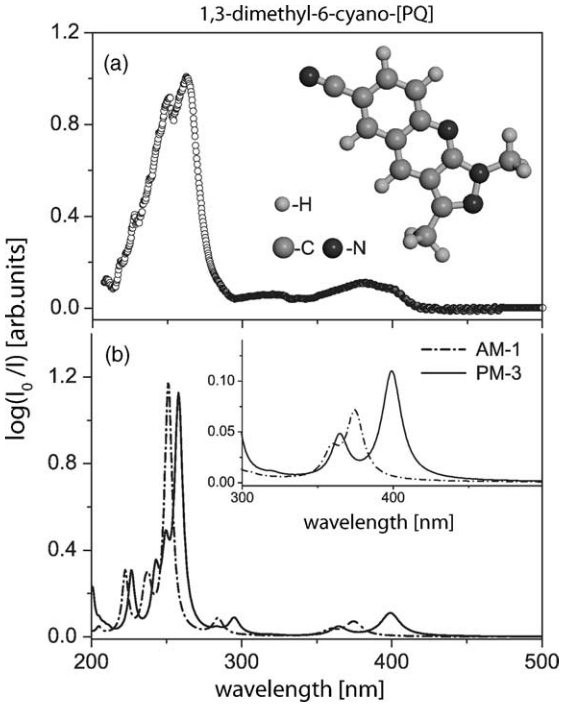

Fig. 3. (a) Measured absorption spectra of 1,3-dimethyl-6-cyano-[PQ] and (b) calculated spectra within the semi-empirical quantum–chemical PM3 and AM1 models. Insert shows the chemical structure of 1,3-dimethyl-6-cyano-[PQ] obtained within the geometrical optimization procedure.

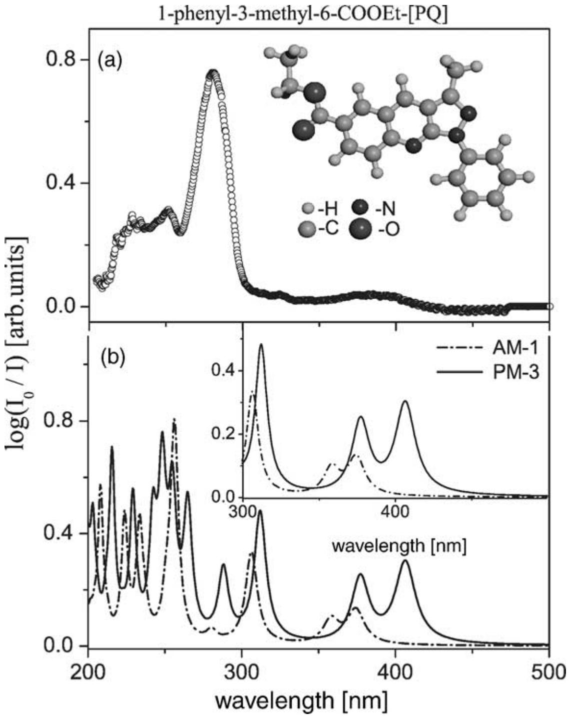

Fig. 4. (a) Measured absorption spectra of 1-phenyl-3-methyl-6-COOEt-[PQ] and (b) calculated spectra within the semi-empirical quantum–chemical PM3 and AM1 models. Insert shows the chemical structure of 1-phenyl-3-methyl-6-COOEt-[PQ] obtained within the geometrical optimization procedure.

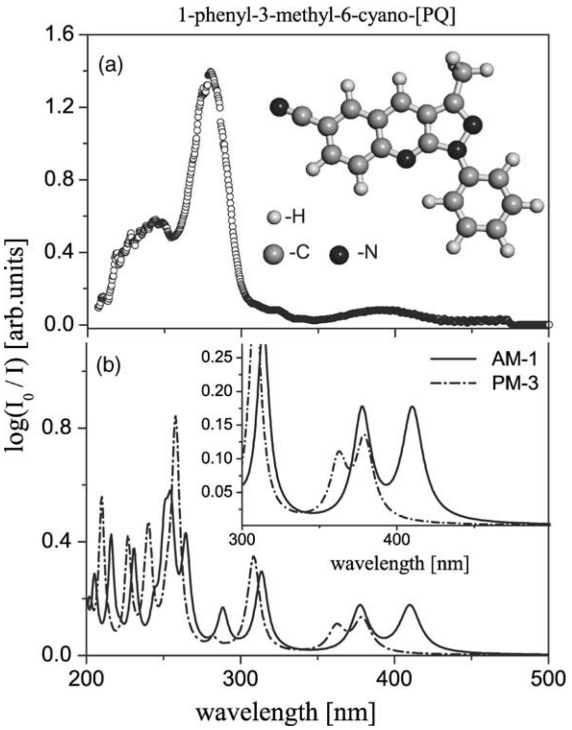

Fig. 5. (a) Measured absorption spectra of 1-phenyl-3-methyl-6-cyano-[PQ] and (b) calculated spectra within the semi-empirical quantum–chemical PM3 and AM1 models. Insert shows the chemical structure of 1-phenyl-3-methyl-6-cyano-[PQ] obtained within the geometrical optimization procedure.

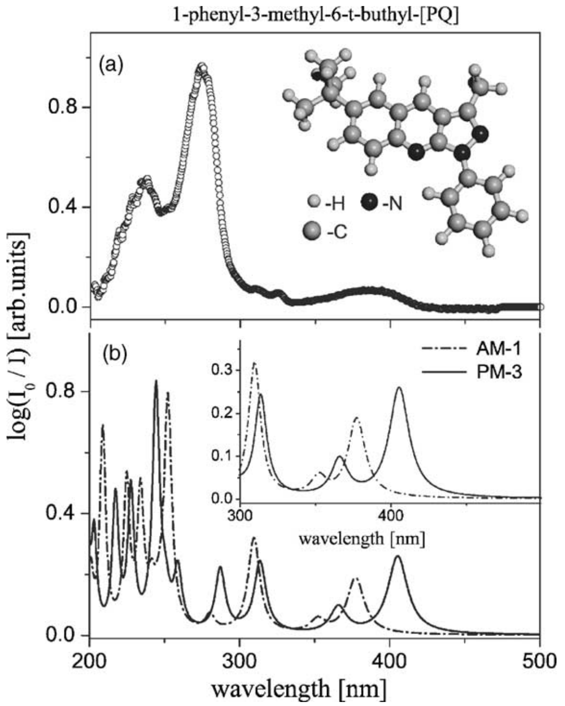

Fig. 6. (a) Measured absorption spectra of 1-phenyl-3-methyl-6-t-buthyl-[PQ] and (b) calculated spectra within the semi-empirical quantum–chemical PM3 and AM1 models. Insert shows the chemical structure of 1-phenyl-3-methyl-6-t-buthyl-[PQ] obtained within the geometrical optimization procedure.

3-methyl-6-cyano-[PQ] and 1-phenyl-3-methyl-6-*t*-buthyl-[PQ], respectively. In addition, the experimental spectra in UV region is characterized by only two/three broad absorption bands. The most strongest bands appear at about 276–280 nm, i.e. are clearly shifted for all compounds to the red region with respect to the position of the series of most intense absorption bands obtained by the quantum–chemical simulations.

The reasons for the discrepancies observed between the measured and calculated spectra of the [PQ]-derivatives have been attributed initially [7] to the solvatochromic effect [15]. Later on, the experiment with strongly and weakly polar solvents (see [8]) have indicated indeed rather small its influence on the absorption spectra. All the solutions clearly have shown only a weak blue shift of λ_g as the solvent polarity increased. A substantial broadening of spectral bands as well as their spectral shifts are, therefore, rather a result of two other eventual mechanisms which are not considered in our quantum–chemical calculations. The first one is the electron–vibronic coupling. Indeed, the lowest energy absorption band reveals features very similar to vibronic replica [see e.g. Figs. 2(a) and 3(a)]. The second mechanism is actual for the [PQ]-derivatives containing methyl, phenyl or *t*-buthyl groups. One should be emphasized that our quantum–chemical calculations have been performed for isolated molecules in vacuum. The optimization procedure gives here a planar molecular configuration for all the [PQ]-derivatives. This is likely not quite correct for solutions where the methyl, phenyl or *t*-buthyl groups are presumably to rotate dynamically affecting the symmetry selection rules for different electronic transitions.

The experimental efficiency of second-order optical susceptibility d versus photoinduced power density I_p for is shown for each chromophore in the Fig. 7. One can see that the efficiency d clearly saturates to certain magnitude d_{eff}

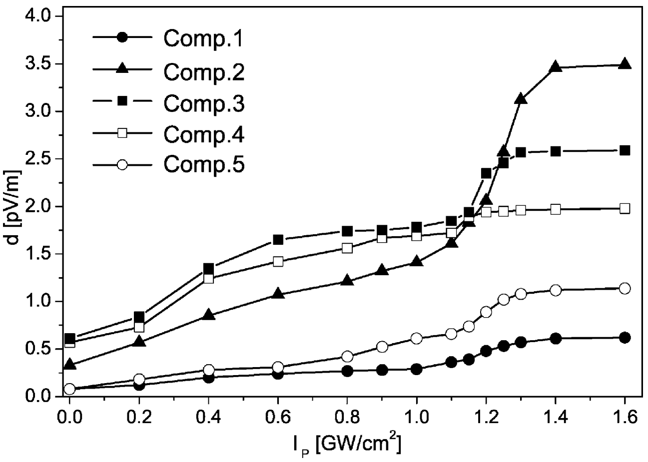

Fig. 7. Efficiency of second-order optical susceptibility d vs photoinduced power density. Comp.1: 1,3-dimethyl-6-COOEt-[PQ]; Comp.2: 1,3-dimethyl-6-cyano-[PQ]; Comp.3: 1-phenyl-3-methyl-6-COOEt-[PQ]; Comp.4: 1-phenyl-3-methyl-6-cyano-[PQ]; Comp.5: 1-phenyl-3-methyl-6-t-buthyl-[PQ].

Table 2
Saturated second-order optical susceptibility d_{eff}, calculated dipole moment $|\vec{p}|$ and calculated effective (averaged) molecular optical nonlinear constant β_{av}

Compound	d_{eff} [pm V^{-1}] (exp.)	$\lvert\vec{p}\rvert$ [D] (AM1)	$\lvert\vec{p}\rvert$ [D] (PM3)	β_{av} [au] (AM1)	β_{av} [au] (PM3)	M_{g} [D] (AM1)	M_{g} [D] (PM3)
Comp.1	0.62	0.652	1.13	56.4	211.9	3.26	4.875
Comp.2	3.49	2.610	2.751	53.1	343.3	4.761	6.776
Comp.3	2.59	3.072	2.463	400.0	681.5	3.507	4.920
Comp.4	1.98	2.14	2.319	330.7	455.3	5.133	7.358
Comp.5	1.14	2.961	2.511	295.8	452.9	0.673	1.635

Comp.1: 1,3-dimethyl-6-COOEt-[PQ]; Comp.2: 1,3-dimethyl-6-cyano-[PQ]; Comp.3: 1-phenyl-3-methyl-6-COOEt-[PQ]; Comp.4: 1-phenyl-3-methyl-6-cyano-[PQ]; Comp.5: 1-phenyl-3-methyl-6-*t*-buthyl-[PQ].

at sufficient power densities ($I_{\mathrm{p}} \geq 1.3$ GW/cm^2). Table 2 lists the saturated second-order optical susceptibility d_{eff} (as obtained from the data presented in the Fig. 7) as well as the dipole moments $|\vec{p}|$, effective (averaged) molecular optical nonlinear constant β_{av} and excited state dipole moments $M_g = \sqrt{M_{\mathrm{g1}}^{(x)2} + M_{\mathrm{g1}}^{(y)2} + M_{\mathrm{g1}}^{(z)2}}$ corresponding to the first active oscillator (as calculated within semiempirical AM1 i PM3 methods). From the data presented one can clearly see that there exists a good correlation between the magnitude of saturated susceptibilities d_{eff} and macroscopic hyperpolarizabilities for all compounds except the chromophore 1,3-dimethyl-6-cyano-[PQ] (Comp.2). It may reflect a specyfic contribution of surrounding polymer matrix for the two methyl-cyano compounds. A substitution a methyl group by the aromatic group probably scatter the corresponding charge transfer thus reducing d_{eff}. In this case the maximally achieved d_{eff} for Comp.2 likely indicates on polarizable effects of guest molecules.

5. Conclusion

In conclusion, we present here results of experimental studies and quantum chemical simulations of optical poling effect and optical absorption performed on a new synthesized cyan, ethylcarboxyl and *tert*-buthyl derivatives of 1H-pyrazolo[3,4-b]quinoline incorporated into polymer matrix or dissolved in organic solutions. The efficiency of second-order optical susceptibility d versus photoinduced power density I_{p} clearly saturates to certain magnitude d_{eff} at sufficient power densities ($I_{\mathrm{p}} \geq 1.3\,\mathrm{GW\,cm^{-2}}$). Comparing experimental data and results of semiempirical quantum–chemical simulations one can conclude that there exists generally a good correlation between the magnitude of saturated susceptibilities d_{eff} and macroscopic hyperpolarizabilities for all compounds except the chromophore 1,3-dimethyl-6-cyano-[PQ] only. The discrepancy for this compound may reflect a specific contribution of surrounding polymer matrix.

The quantum–chemical analysis reveals similarity in the absorption spectra of methyl-containing derivatives which are characterized by four or five strong absorption bands in the spectral range 200–500 nm. A substitution of the methyl groups by the phenyl group causes the substantial changes of the absorption spectra mainly in the spectral range 240–370 nm. We attribute these differences to additional molecular double bonding segments C=C of the substituted phenyl groups, thereby the electronic $\pi \rightarrow \pi^*$ transitions appear to be involved into the absorption process. The comparison of measured and calculated absorption spectra manifests rather good agreement, namely in the part regarding the spectral positions of the first oscillator (absorption threshold). At the same time, the measured spectra reveal the considerable broadening almost of all absorption bands and even complete damping some of them in the case of phenyl derivatives. The discrepancies between the calculated and the measured spectra are attributed to electron–vibronic coupling as well as to specific rotational dynamics of phenyl rings.

Acknoledgements

This work was supported by KBN grant no. 3-T11-B-074-26.

References

[1] M.K. Balakirev, I.V. Kityk, V.A. Smirnov, L.I. Vostrikova, J. Ebothe, Phys. Rev. A 67 (2003) 023806.
[2] I.V. Kityk, M. Makowska-Janusik, E. Gondek, L. Krzeminska, A. Danel, K.J. Plucinski, S. Benet, B. Sachraoui, J. Phys. Cond. Matt. 16 (2004) 231.
[3] B.P. Antonyuk, Optics Commun. 174 (2000) 427.
[4] Z. He, G.H.W. Milburn, K.J. Baldwin, D.A. Smith, A. Danel, P. Tomasik, J. Lumin. 86 (2000) 1.
[5] Z. He, G.H.W. Milburn, A. Danel, A. Puchala, P. Tomasik, D. Rasala, J. Mater. Chem. 7 (1997) 2323.
[6] A. Danel, Z. He, G.H.W. Milburn, P. Tomasik, J. Mater. Chem. 9 (1999) 339.
[7] E. Koscien, J. Santra, E. Gondek, A. Danel, A. Wisla, A.V. Kityk, Optics Communications 227 (2003) 115.
[8] E. Gondek, E. Koscien, J. Santra, A. Danel, A. Wisla and A. V. Kityk, Spectrochi. Acta, Part A, in press.
[9] J. Becher, B.F. Hansen, N. Malhotra, J. Heterocycl. Chem. 28 (1991) 1837.
[10] L. Hennig, T. Müller, M. Grosche, J. Prakt. Chem. 332 (1990) 693.
[11] A. Danel, K. Chaczatrian, P. Tomasik, ARKIVOC 1 (2000) 51.
[12] A. Danel, PhD Thesis, Synthesis 1H-pyrazolo[3,4-b]quinolines as a luminofores for LED’s, (1996).
[13] I.V. Kityk, B. Marcinzak, A. Mefleh, J. Phys. D: Appl. Phys. 34 (2001) 1.
[14] R. Boyd, Principles of Nonlinear Optics, Academic Press, NY, 1983.
[15] C. Reichardt, Solvents and Solvent Effects in Organic Chemistry, VCH Verlagsgesellschaft mbH, D-6940 Weinheim, Germany, 1988.